Plant Science 316 (2022) 111155

Contents lists available at ScienceDirect

Plant Science

journal homepage: www.elsevier.com/locate/plantsci

A rice tubulin tyrosine ligase like 12 regulates phospholipase D activity and tubulin synthesis

Kunxi Zhang [a], Wenjing Shi [b], Xin Zheng [a], Xuan Liu [a], Lixin Wang [b], Michael Riemann [a], Dimitri Heintz [c], Peter Nick [a,*]

[a] Molecular Cell Biology, Botanical Institute, Karlsruhe Institute of Technology, Fritz-Haber-Weg 4, 76131, Karlsruhe, Germany
[b] College of Horticulture, Hebei Agricultural University, Baoding, 071001, Hebei, China
[c] Plant Imaging and Mass Spectrometry (PIMS), Institut de Biologie Moléculaire des Plantes, Centre National du Recherche Scientifique (CNRS-IBMP), Université de Strasbourg, 12 rue du Général Zimmer, 67084, Strasbourg, France

ARTICLE INFO

Keywords:
Detyrosination
Microtubule
Phospholipase D
Tubulin tyrosine carboxypeptidase
Tubulin tyrosine ligase like 12
Tyrosination

ABSTRACT

All plant α-tubulins encode a C-terminal tyrosine. An elusive tubulin tyrosine carboxypeptidase can cleave off, and a tubulin tyrosine ligase (TTL) re-ligate this tyrosine. The biological function of this cycle remains unclear but may correlate with microtubule stability. To get insight into the functional context of this phenomenon, we used cold-induced elimination of microtubules as experimental model. In previous work, we had analysed a rice TTL-like 12 (OsTTLL12), the only potential candidate of plant TTL. To follow the effect of OsTTLL12 upon microtubule responses *in vivo*, we expressed OsTTLL12-RFP into tobacco BY-2 cells stably overexpressing NtTUA3-GFP. We found that overexpression of OsTTLL12-RFP made microtubules disappear faster in response to cold stress, accompanied with more rapid Ca^{2+} influx, culminating in reduced cold tolerance. Treatment with different butanols indicated that α-tubulin detyrosination/tyrosination differently interacts with phospholipase D (PLD) dependent signalling. In fact, rice PLDα1 decorated microtubules and increased detyrosinated α-tubulin. Unexpectedly, overexpression of the two proteins (OsTTLL12-RFP, NtTUA3-GFP) mutually regulated the accumulation of their transcripts, leading us to a model, where tubulin detyrosination feeds back upon tubulin transcripts and defines a subset of microtubules for interaction with PLD dependent stress signalling.

1. Introduction

Microtubules are composed of α- and β- tubulin heterodimers. These heterodimers form a highly dynamic structure that exhibits both growth at the plus-end and shrinking at the minus-end at the same time. The transition between growth and shrinkage, so called dynamic instability, forms the basis for the organisation and remodelling of microtubules [1]. This unique feature of microtubules endows them with diverse functions. For instance, the orientation of cortical microtubule arrays defines the directional cell expansion, while different mitotic microtubule arrays control axis and symmetry of cell division. Both processes allow a control of plant shape.

In addition to these classical functions in morphogenesis, stability and re-organisation of microtubules participate in the sensing of cold stress [2]. Among the numerous physiological and molecular events for cold sensing, signal transduction and adaptive responses, culminating in cold tolerance, the rapid elimination of microtubules represents one of the early responses, preceding changes of gene expression [2]. Efficient cold acclimation correlates with a rapid, but transient elimination of microtubules, a phenomenon occurring both in winter wheat [3] and in grapevine cells [4]. In both systems, this can be mimicked in absence of cold stress by pronamide, a mild microtubule eliminating compound. This demonstrates that the rapid elimination of microtubules is sufficient to activate cold acclimation. On the other hand, stabilisation of microtubules by taxol can improve acclimation as well [4]. These seemingly paradox functions of microtubules derive from different subpopulations that differ in dynamics and with respect to their role in cold signalling [2]. While stable microtubules act as susceptors to collect and amplify the physical input from cold-induced membrane rigidification, dynamic microtubule arrays are needed as well to integrate vesicles that contain signalling compounds into plasma membrane. When different microtubule populations do different jobs, because their dynamics differ, this leads to the question, how these populations are assigned on the molecular level.

* Corresponding author.
E-mail address: peter.nick@kit.edu (P. Nick).

https://doi.org/10.1016/j.plantsci.2021.111155
Received 3 August 2021; Received in revised form 27 October 2021; Accepted 11 December 2021
Available online 16 December 2021

It is generally believed that the stability of microtubules is regulated by a great variety of microtubule associated proteins (MAPs), responsible regulation of microtubule assembly and organisation [5]. One of these MAPs is the enzyme phospholipase D (PLD), a 90 kDa protein which can be isolated from membrane fraction of tobacco BY-2 cells, and which decorates cortical microtubules and, thus, likely acts as a cross-bridge between cortical microtubule and plasma membrane [6,7]. Treatment with *n*-butanol, which interferes with the accumulation of phosphatidic acids, products of PLD with signal activity, eliminates cortical microtubules. The functional context of this interaction between PLD and microtubules might be the sensing and processing of stress signals, especially cold stress [2]. Indeed, activation of PLD is necessary for the microtubule response to cold as shown by experiments using different butanols in a grapevine cell line, where microtubules were tagged by GFP [8]. Also for the response of *Arabidopsis thaliana* to heat shock, activation of a specific isotype of the enzyme, PLDδ and an initial microtubule elimination are important to induce heat acclimation [9]. These findings place PLD in a position upstream of cortical microtubules in the processing of thermal stress. This sensory function depends on specific subpopulations of microtubules that differ with respect to their dynamics [10]. However, how these specific subpopulations of microtubules are delineated, has remained elusive.

Promising candidates for such a molecular delineation event are posttranslational modifications of α- and β- tubulins since they associate with differences in stability and structure of microtubules. The most common posttranslational modification is the cycle of α-tubulin detyrosination and re-tyrosination by enzymatic removal and re-ligation of the C-terminal tyrosine. The enzyme tubulin tyrosine ligase (TTL), responsible for ligation of C-terminal tyrosine has been identified firstly in neural tubulins [11], while the tubulin tyrosine carboxypeptidase (TCP) that removes C-terminal tyrosine has been identified only recently, as vasohibins and small vasohibin binding proteins [12,13]. It should be mentioned that plant lack any homologues for vasohibins, nor small vasohibin-binding proteins. Nevertheless, they are endowed with a tubulin tyrosine carboxypeptidase function (in plants often abbreviated as TTC). While TTL preferentially binds to free tubulin heterodimers [14], TCP/TTC has a higher affinity for assembled microtubules [15]. As a result, tyrosinated α-tubulin is enriched in dynamic microtubules, whereas stable microtubules harbour more detyrosinated α-tubulin. This correlation between stability and detyrosination seems to be valid for plants as well, as shown for auxin-dependent reorientation of cortical microtubules in maize coleoptiles [16]. In cold acclimation of winter wheat, the sensory function of microtubules during the response to cold stress requires a rapid, but transient elimination linked with high dynamics. These becomes manifest as an increased tyrosination of α-tubulin, while the cold-stable microtubule arrays that form later in consequence of cold-hardening are mostly detyrosinated [3]. These findings indicate that α-tubulin detyrosination and tyrosination might define different subpopulations with different dynamics and functions during cold sensing.

However, TTC, the enzyme responsible for detyrosination has remained still elusive. Moreover, while TTL occurs in gene families in animals, where canonical TTLs co-exist with several TTL-like proteins that participate in various tubulin modifications [17], in plants, there are only homologues of TTL-like 12 proteins, which, therefore, qualify as most likely plant candidates for putative TTLs [18]. In fact, when we overexpressed the rice TTL-like 12 (OsTTLL12) in rice and in tobacco cells [18], we observed that tubulin detyrosination and tyrosination were modulated, which coincided with changes in cell and organ growth, but also with perturbations in the orientation of the phragmoplast, a plant-specific microtubule structure guiding the orientation of the cross wall after mitosis. To find out, whether post-translational modification of specific microtubule subpopulations play a role in cold sensing, we overexpressed the OsTTLL12 fused with RFP in the background of a tobacco BY-2 microtubule marker cell line overexpressing NtTUA3-GFP. We find that overexpression of OsTTLL12-RFP resulted in reduced cold tolerance, which correlated with rapid depolymerisation of microtubules and elevated cold-induced Ca^{2+} influx. We also find evidence for differential interaction of microtubules with PLD depending on their tyrosination or detyrosination status. Unexpectedly, we also detect a feedback of detyrosination and tyrosination levels on the expression of α-tubulin, acting on the post-transcriptional level. We arrive at a model, where microtubule dynamics not only modulates cold sensing, but also participates in a homeostatic loop calibrating tubulin synthesis with microtubule turnover.

2. Materials and methods

2.1. Generation of transgenic tobacco BY-2 cell lines

To get the stable transformation of OsPLDα1-GFP BY-2 cell line, total RNA was firstly isolated from coleoptiles of *Oryza sativa* ssp. *japonica* cv. Dongjin by using the innuPREP Plant RNA kit (Analytik Jena, Jena, Germany). After reverse transcription by the M-MuLV cDNA Synthesis Kit (New England Biolabs) according to the instructions of the manufacturer. The full-length coding sequence of OsPLDα1 (Accession number: LOC4327647) was amplified from cDNA template by PCR using the oligonucleotide primers: *attB*1-PLD (forward primer): 5′-GGGGACAAGTTTGTACAAAAAAGCAGGCTTCATGGCGCAGATGCTGCTCCATG-3′

and *attB2*-PLD (reverse primer): 5′-GGGGACCACTTTGTACAAGAAAGCTGGGTTCTATGAGGTGAGGATGGGGGGCATG-3′ with initial denaturation at 94 °C for 7 min, followed by 30 cycles of denaturation at 94 °C for 1 min, annealing at 60 °C for 1 min, and elongation at 72 ° for 2 min, terminated by a final elongation step at 72 °C for 4 min. Then, the PCR amplicon was integrated into the entry plasmid pDONR/Zeo (Invitrogen), which after verification of the sequence, was then cloned into the binary GATEWAY vector pK7W6F2. This vector allows for N-terminal fusion of the green fluorescent protein, driven by the constitutive CaMV 35S promoter, and followed by kanamycin resistance. After verification of the sequence, the vector was then ready for stable transformation into tobacco BY-2 cell (*Nicotiana tabacum* L. cv Bright Yellow 2) using an *Agrobacterium*-mediated protocol as described in [18]. The non-transformed tobacco BY-2 cell was referred to as WT BY-2.

To follow the localisation of OsTTLL12 in relation to microtubules, the microtubule marker line NtTUA3-GFP BY-2 [19] was transformed with the vector pH7WGR2-OsTTLL12 [18] using an *Agrobacterium*-mediated protocol as described in [18]. This vector harbours the coding fusion of OsTTLL12: LOC_Os03 g08140 behind the red fluorescent protein, driven by the constitutive CaMV 35S promoter, and followed by a hygromycin resistance in a stable manner. This line overexpressing both, OsTTLL12-RFP and NtTUA3-GFP, was referred to as TTLL12 + TUA3 cell line, to distinguish it from the microtubule marker line NtTUA3-GFP BY-2 which for brevity is designated as TUA3 line.

2.2. Cultivation of tobacco BY-2 cells and plant materials

The WT BY-2 cell line, along with the transformed BY-2 cell lines used in this work were cultivated in Murashige-Skoog medium, containing 4.3 g/L Murashige and Skoog salts (Duchefa, Haarlem, The Netherlands), 30 g/L sucrose, 200 mg/L K_2HPO_4, 100 mg/L *myo*-inositol, 1 mg/L thiamine and 0.2 mg/L 2,4-dichlorophenoxyacetic acid (2,4-D), pH 5.8. For the transgenic lines, the medium was supplemented with the appropriate antibiotics (OsTTLL12-RFP [18] with 30 mg/L hygromycin); OsPLDα1-GFP and TUA3 with 50 mg/L kanamycin; TTLL12 + TUA3 with both 30 mg/L hygromycin and 50 mg/L kanamycin). The cells grew under continuous shaking at 150 rpm, at 25 °C in darkness. The cells were subcultured either weekly (WT BY-2, OsTTLL12-RFP and OsPLDα1-GFP) or bi-weekly (TUA3 and TTLL12 + TUA3) by inoculating 1.5 mL of stationary cells into fresh medium (30

mL) in 100 mL flasks.

Etiolated coleoptiles were raised from an line of *Oryza sativa* ssp. *japonica* cv. 'Dongjin' overexpressing rice phospholipase Dα1 fused with GFP [20] along with non-transformed plants from the same variety. After equidistant sowing, the caryopses were cultivated on a polyurethane mesh floating 100 mL ddH_2O in a Plexiglass box at 25 °C in photobiological darkness as described by [18].

2.3. Cold stress treatment of tobacco BY-2 cells

To administer cold stress, aliquots of the cell suspension in 2 mL Eppendorf tubes (Eppendorf, Hamburg) were submerged into an ice-water bath (0 °C) and shaken in the dark on a horizontal shaker as described in [8] using cells of lines TUA3 and TTLL12 + TUA3 BY-2 collected at day 7 after subcultivation.

2.4. Measuring extracellular alkalinisation

Before applying cold stress, 4 mL of suspension cells for lines WT, OsTTLL12, TUA3 and TTLL12 + TUA3 BY-2 were first pre-equilibrated at 25 °C on an orbital shaker for 30 min. After incubation in ice-water for 60 min, the cells returned to room temperature for one additional hour. Throughout the entire experiment, including pre-equilibration, cold treatment, and recovery from cold-treatment, the extracellular pH was recorded by a pH meter (Schott handy lab, pH 12) combined with a pH electrode (Mettler Toledo, LoT 403-M8-S7/120) coupled to a paperless readout (VR06; MF Instruments GmbH, Albstadt-Truchtelfingen, Germany).

2.5. Determination of cell mortality

After cold treatment for 24 h, we measured mortalities of WT, OsTTLL12, TUA3 and TTLL12 + TUA3 cells by the Evans Blue Dye Exclusion Test in 1 mL of 2.5 % (w/v) Evans Blue (Sigma-Aldrich) as described in [4], using custom-made staining chambers to remove the medium. After washing 3 times with ddH_2O for 5 min, we scored the number of dead (blue) cells in a population of 500 cells per replicate using an AxioImager Z.1 microscope (Zeiss, Jena, Germany) as described in [4]. Cell mortality was determined as ratio of dead cells over total cell count. Data represent the values pooled from three independent experimental series, representing 1500 individual cells.

2.6. Oryzalin and taxol treatment

To test the effects of oryzalin and taxol on steady-state transcript levels for the transgenes OsTTLL12 and NtTUA3, stationary cells of lines TUA3 and TTLL12 + TUA3 BY-2 were treated at day 7 after subcultivation with 5 μM oryzalin or 5 μM taxol. The solvent control consisted in the equivalent volume of DMSO. After oryzalin treatment for 2 h under continuous shaking at 150 rpm in the dark, the cells were harvested and stored in liquid nitrogen till extraction of RNA.

2.7. Actinomycin D and cycloheximide treatment

To block transcription, we used Actinomycin D [21] at 50 μg/mL diluted from a stock of 1 mg/mL in 50 % EtOH along with the equivalent of 50 % EtOH as solvent control. To inhibit translation, we used Cycloheximide [22] at 100 μg/mL diluted from an aequous stock of 10 mg/mL. Treatment lasted for 2 h, continuously shaking at 150 rpm in the dark, before the cells were harvested and stored in liquid nitrogen till extraction of RNA.

2.8. Treatment with different butanols and $GdCl_3$

To test for a potential role of phospholipase D signalling in the microtubular response, the formation of phosphatidic acids was outcompeted using 1% *n*-butanol for 1 h [23]. Treatment with 1% *sec*-butanol, and 1% *tert*-butanol, respectively, served as negative control. We followed the microtubular responses to these compounds under control temperatures, and in combination with cold stress in stationary cells of lines TUA3 and TTLL12 + TUA3, respectively.

To test the requirements of calcium influx on cold-induced microtubules depolymerisation, 150 μM $GdCl_3$ was applied to prevent the calcium influx as described in [8]. The TUA3 and TTLL12 + TUA3 cell lines were pre-treated with 150 μM $GdCl_3$ for 30 min at room temperature before transfer to cold stress (°C) and then we followed the microtubular responses in a time series 0, 5 and 15 min under cold stress.

2.9. RNA extraction, cDNA synthesis and real-time PCR

To probe for gene expression, we used lines OsTTLL12-RFP BY-2, TUA3 and TTLL12 + TUA3 at the transition between proliferation and cell expansion phase. Since lines TUA3 and TTLL12 + TUA3 progress more slowly, this time point was at day 7 after subcultivation, while for the more rapid OsTTLL12-RFP, this transition occurred earlier, at day 4 after subcultivation. The three lines were either treated with 5 μM oryzalin or with 5 μM taxol for two hours or kept untreated. After removing the medium by a Büchner funnel *via* short-time vacuum (10 s), the cells were collected in a 2 mL Eppendorf tube, immediately frozen in liquid nitrogen, and homogenised with a Tissue Lyser (Qiagen/Retsch Hilden, Germany). Total RNA was isolated using the innuPREP Plant RNA kit (Analytik Jena, Jena, Germany) according to the instructions of the manufacturer. The quality of extracted RNA was verified by electrophoresis on a 1.0 % agarose gel that mixed with 0.6x MIDORI Green Xtra (Nippon Genetics) and visualised on a Safe Imager blue light transilluminator (Invitrogen, Germany). Reverse transcription into cDNA was conducted with the M-MuLV cDNA Synthesis Kit (New England Biolabs) according to the instructions of the manufacturer using 1 μg of total RNA as template. Real-time PCR was performed by using a Bio-Rad CFX detection System (Bio-Rad, USA) and the quantitative relative expression level of OsTTLL12 and NtTUA3-GFP was calculated with the $2^{-\Delta\Delta Ct}$ method [24] using L25 ribosomal protein [25] as internal reference genes for normalisation. Supplementary Table 1 lists the details of the oligonucleotide primers used in this study.

2.10. Protein extraction and Western blot

The cells overexpressing OsPLDα1-GFP (at day 5 after subcultivation), the TUA3 cells and the TTLL12 + TUA3 lines (both at day 7 after sub-cultivation) were harvested by a Büchner funnel *via* short-time vacuum (10 s) under room temperature. Then, the cells were transferred into an ice-cold mortar and ground to a fine powder with a pestle. Proteins were extracted by adding the same volume of cold extraction buffer (25 mM MES, 5 mM EGTA, 5 mM $MgCl_2{\cdot}6H_2O$, pH 6,9 adjusted by KOH, 1 mM DTT and 1 mM PMSF), and vigorously mixed as described in [18]. After centrifugation at 13,500 rpm for 30 min at 4℃, the sediment that contained cell wall debris and other insoluble remains was discarded and the soluble protein in the supernatant was collected.

Protein extracts were then denatured at 95℃ for 5 min and spun down at 13,500 rpm for 30 min under room temperature. Equal amount of protein samples was loaded to two sets of SDS-PAGE on 10 % (w/v) polyacrylamide gels: one set was used for Coomassie Brilliant Blue staining to verify the equal loading of lanes, while the other set was used for Western blot, detecting detyrosinated or tyrosinated α-tubulin as well as GFP fused TUA3 protein and β-tubulin. Pre-stained size markers (P7704S or P7712S, New England Biolabs) were loaded as well and used as a molecular weight standard. To detect tyrosinated and detyrosinated α-tubulin and β-tubulin, we used the monoclonal antibodies ATT (T9028, Sigma-Aldrich, Darmstadt, Germany) and DM1A (T9026, Sigma-Aldrich, Darmstadt, Germany) and DM1B (ab9267, Sigma-Aldrich, Germany), respectively [18], in a dilution of 1:2000 in TBS buffer containing 20 mM Tris−HCl, pH 7.6 and 150 mM NaCl. To detect

GFP fusions with tobacco TUA3, we used the monoclonal anti-GFP antibody directed against a C-terminal peptide specific for GFP (mouse clone GSN149, Sigma-Aldrich, Germany) was used at a dilution of 1:2000 in TBS buffer. The signal was visualised with a polyclonal anti-mouse IgG coupled with alkaline phosphatase (Sigma-Aldrich, Germany), applied at a dilution of 1:30000 in TBS buffer.

2.11. Microtubule visualisation and microscopy

Cortical microtubules were fluorescent though the GFP tagged microtubule marker NtTUA3 in lines TUA3 and TTLL12 + TUA3. This allowed following their responses to various chemical treatments and cold stress by spinning-disc confocal microscopy, collecting image z-stacks as described in [8]. To assess the localisation of OsPLDα1-GFP with microtubules, microtubules were stained by immunofluorescence using a monoclonal anti-α-tubulin (DM1A, diluted 1:100, Sigma-Aldrich, Deisenhofen, Germany) as primary antibody, and a TRITC conjugated anti-mouse IgG antibody (diluted 1:20, Sigma-Aldrich, Deisenhofen, Germany) as secondary antibody. Microtubules were visualised in either cycling cells of the tobacco BY-2 cell line overexpressing OsPLDα1-GFP, or in etiolated coleoptiles of the overexpressing OsPLDα1-GFP rice line, as described in [18]. In case of the GFP-tagged microtubules, time-lapse series of individual cells were recorded every 30 min under a spinning disc confocal microscope equipped with a cooled digital CCD camera (AxioCamMRm; Zeiss), and the 488-nm and 561-nm lines of an Argon-Krypton laser (Zeiss, Jena, Germany) to record the GFP and the TRITC signals, respectively.

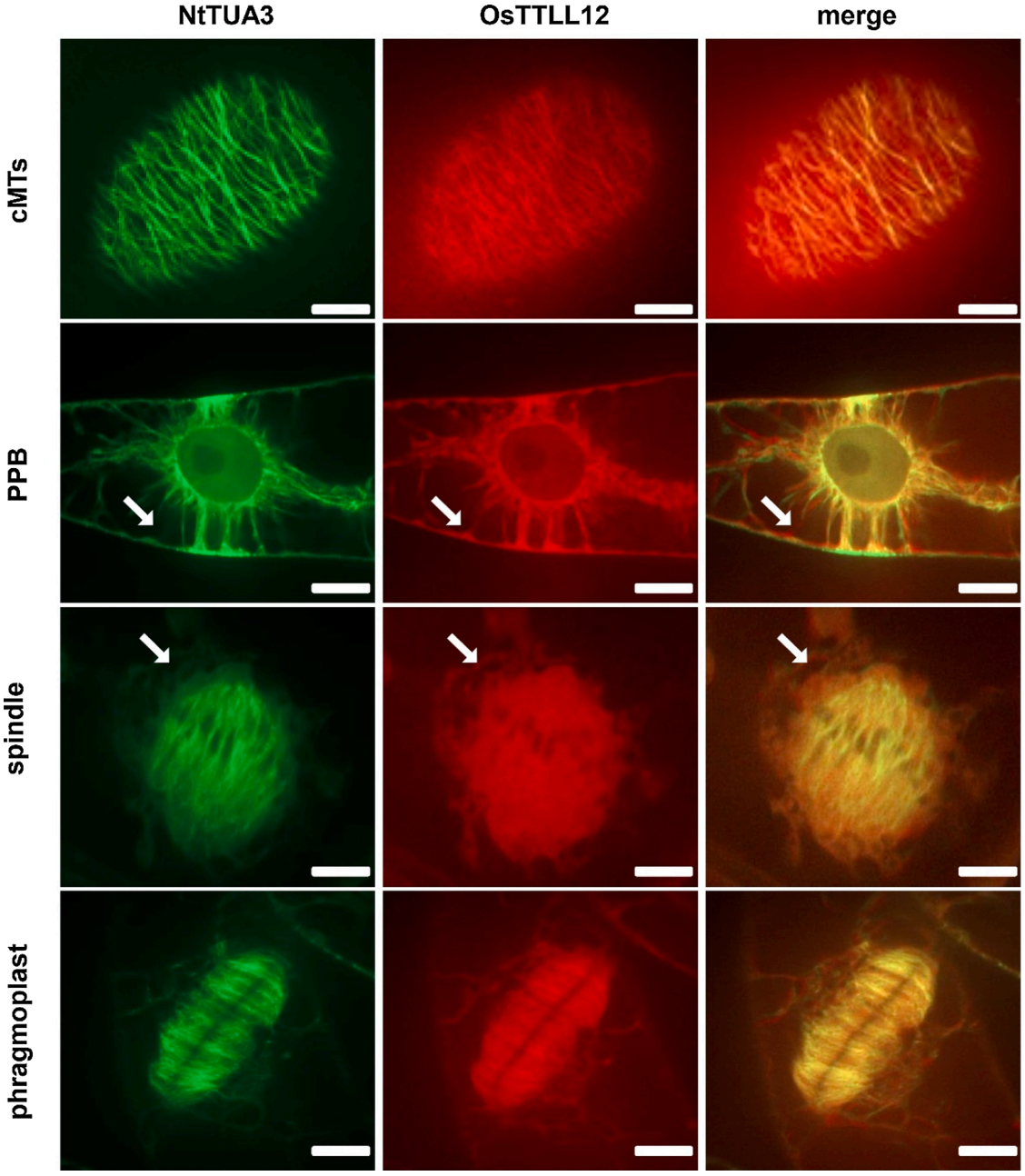

Fig. 1. Localisation of OsTTLL12 on different microtubule arrays in tobacco BY-2 cells. Cells overexpressing OsTTLL12-RFP and the microtubule marker NtTUA3-GFP were analysed at different stages of the cell cycle by spinning disc confocal microscopy. **a**, cortical microtubules in G1 interphase cells; **b**, preprophase band (PPB) in G2 cells; **c**, mitotic spindle in late metaphase; **d**, phragmoplast in telophase. Images show geometrical projections of confocal z-stacks. The white arrows indicate, where the OsTTLL12-signalling was independent on microtubules. Size bar: 10 μm.

3. Results

3.1. *OsTTLL12 decorates all microtubule arrays, but also occurs in a free pool*

In our previous work, we had followed the localisation of OsTTLL12-RFP with respect to the different microtubule arrays occurring during the cell cycle using immunofluorescence [18]. This involves permeabilisation of the cells, following chemical fixation. To test, to what extent OsTTLL12 associates with microtubules *in vivo*, we generated a dual marker line expressing OsTTLL12-RFP in the background of the microtubule marker line NtTUA3-GFP. We found that OsTTLL12 decorated all microtubule arrays (Fig. 1), including cortical microtubules in the G_1 phase, the preprophase band (PPB) during the late G_2 phase, spindle microtubules during metaphase, and phragmoplast microtubules during telophase. However, in addition to OsTTLL12 co-localising with microtubules, there was also a smaller, but distinct pool of OsTTLL12 that was not linking to microtubules (Fig. 1, white arrow). For instance, in the longitudinal cytoplasmic strands tethering the nucleus during the late G_2 phase, OsTTLL12 did not decorate microtubules (Fig. 1b). Likewise, in the cytoplasm surrounding the spindle, OsTTLL12 seemed to be detached from microtubules (Fig. 1c). These observations are consistent with our previous findings that the microtubular association of OsTTLL12-RFP appeared very strict upon immunofluorescent labelling, while *in vivo* a significant cytoplasmic signal was masking this association [18]. Notably, after 50 μM taxol treatment, the OsTTLL12-RFP signal became completely diffuse with no clear localisation with cortical microtubules (Supplemental Fig. 1). Since taxol

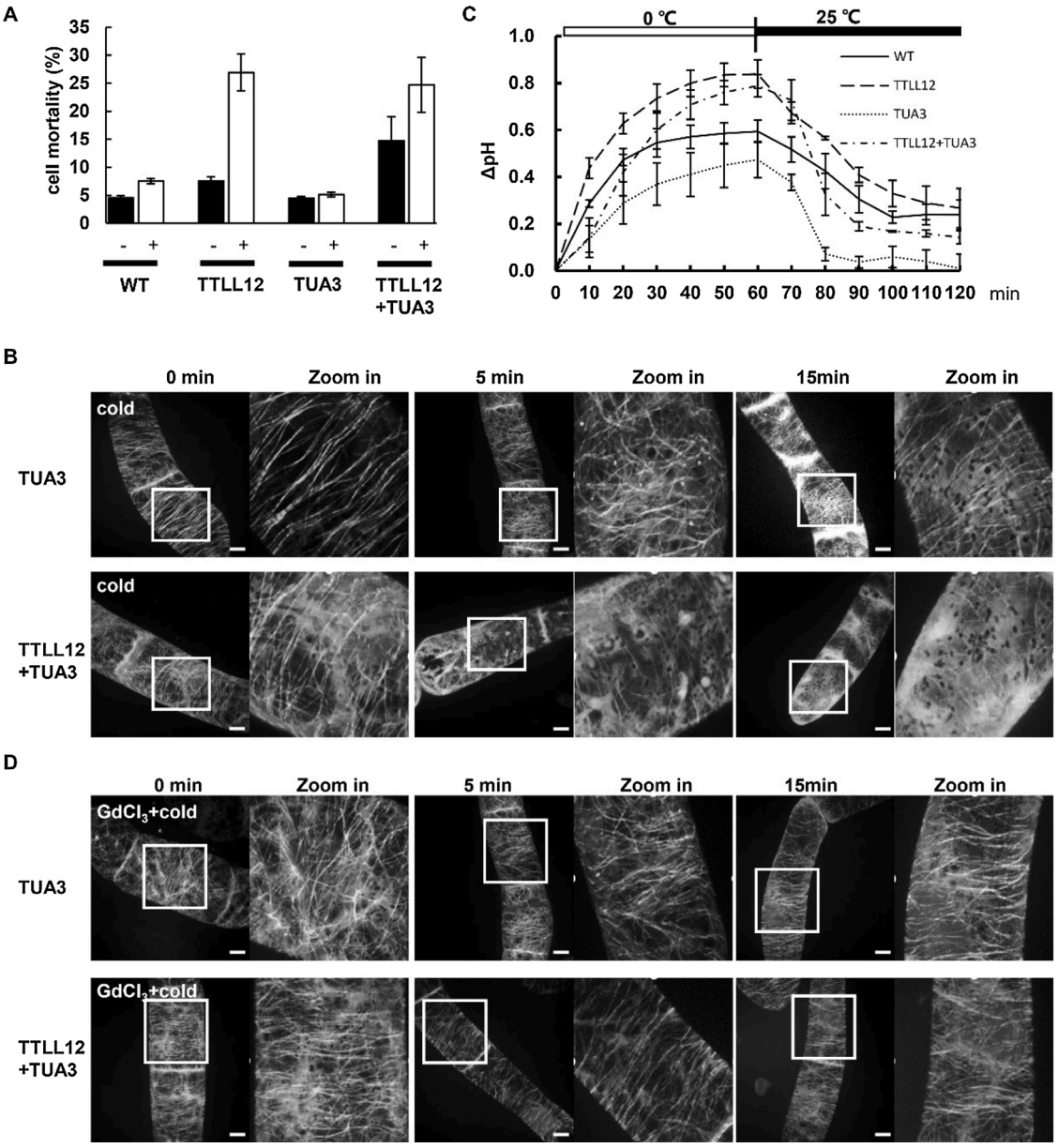

Fig. 2. Effect of TTLL12 overexpression on cold responses in tobacco BY-2 cells. Non-transformed BY-2 cells (WT), cells overexpressing either OsTTLL12-RFP (TTLL12), NtTUA3-GFP (TUA3), or both (TTLL12 + TUA3) were either kept without (-) or with (+) cold stress (0 °C) to assess different cold responses. A, Cell mortality 24 h after the onset of the treatment. Data represent means and standard errors from three independent experiments comprising n = 500 cells per experiment. B, Rapid response of cortical microtubules to cold stress visualised by the marker NtTUA3-GFP either in the absence (upper row) or presence of OsTTLL12-RFP. Size bar: 10 μm. C, Extracellular alkalinisation in response to cold stress for 60 min and recovery at 25 °C room temperature after 60 min to 120 min. Data represent mean values of three independent experiments. D, Effect of 150 μM $GdCl_3$ on the microtubular responses to cold stress (0 °C) visualised by the marker NtTUA3-GFP either in the absence (upper row) or presence of OsTTLL12-RFP.

stablised microtubules that would deplete the free tubulin dimers in the cytoplasm pool, the observed completely diffuse signal of OsTTLL12-RFP indicated that OsTTLL12 requires free of tubulin dimers to enter microtubules.

3.2. Overexpression of OsTTLL12 promotes cold-induced microtubule depolymerisation, calcium influx and cell death

Since OsTTLL12 localises to microtubules and microtubules are reported to be the upstream signalling component in cold stress [2,8], we wondered whether OsTTLL12 would modulate cold responses of microtubules. As first step, we probed for a potential modulation of cold tolerance comparing non-transformed WT BY-2 cells, BY-2 cells stably overexpressing OsTTLL12-RFP (TTLL12), the microtubule marker BY-2 cell line stably overexpressing NtTUA3 (TUA3), and the BY-2 cell line overexpressing both OsTTLL12-RFP and NtTUA3-GFP (TTLL12 + TUA3). We measured cell mortalities after 24 h of cold stress (0 °C). While mortality in WT and TUA3 BY-2 cells was not significantly elevated over the control, the cell mortality of TTLL12 and TTLL12 + TUA3 cell lines were significantly induced by cold stress for 24 h from around 7%–26% in the TTLL12 cell line, and from around 15%–26% in the TTLL12 + TUA3 cell line (Fig. 2A). Thus, overexpression of OsTTLL12 led to reduced cold tolerance, independently of presence or absence of the TUA3 marker.

In the following, we wondered whether this reduced cold tolerance correlated with changes of cold-induced elimination of cortical microtubules due to overexpression of OsTTLL12. Therefore, we followed the response of microtubules to cold stress (0 °C) in the TUA3 and TTLL12 + TUA3 cell lines (Fig. 2B). Without cold, cortical microtubules in TUA3 as well as in TTLL12 + TUA3 cells were mainly oriented as parallel bundles that aligned perpendicular to the long cell axis (Fig. 2B, 0 min). Upon cold stress, cortical microtubules in the TUA3 cell line became thinner, detectable from 5 min, but even after 15 min of cold stress we could still see numerous microtubules, although some had disappeared. Simultaneously, a diffuse background fluorescence appeared in the cytoplasm, probably from fluorescently labelled tubulin heterodimers. The pattern in TTLL12 + TUA3 cells contrasted clearly. Here, already after 5 min of cold stress, only few short remnants of microtubules remained, while the diffuse background fluorescence was dominant (Fig. 2B). Likewise, fluorescence accumulated around the nuclear envelope and at the cross wall. After 15 min, not a single microtubule remained, while fluorescence at the cross walls had become very strong. Thus, upon overexpression of OsTTLL12, cold stress eliminates cortical microtubules more swiftly and more thoroughly.

Calcium is an important second messenger that triggers intercellular processes in response to numerous external stimulus, such as cold, drought and high salinity, and probably involved in transient disruption of cortical microtubules to these stress factors [10,26]. Therefore, we asked whether the more pronounced cold-induced elimination of cortical microtubules in the TTLL12 + TUA3 BY-2 cell line would associate with increased Ca^{2+} influx. To test it, firstly we followed the effects of microtubular responses to cold stress upon 30 min pre-treatment with 150 μm $GdCl_3$, which is a commonly used blocker of calcium influx [8]. We observed that $GdCl_3$ pretreatment for 30 min almost suppressed the cold-induced elimination of cortical microtubules in both TUA3 and TTLL12 + TUA3 cell lines (Fig. 2D, as compared with Fig. 2B), suggesting the rapid cold-induced elimination of cortical microtubules due to overexpression of OsTTLL12 was caused by cold-induced calcium influx. To further test this idea, we followed extracellular alkalinisation as readout of Ca^{2+} influx [27] under cold stress for 60 min and subsequent 60 min of recovery at room temperature. As expected, in all tested BY-2 cell lines, cold stress triggered an extracellular alkalinisation, which dissipated upon re-warming (Fig. 2C). However, we observed distinct differences with respect to the amplitude. In WT BY-2 cells, the pH increased by around 0.5 units during the first 30 min of cold stress and remained stable during the following 30 min of cold stress. Upon transfer to room temperature, pH dropped slowly, but did not return to the initial value, but remained somewhat (by around 0.25 units) more alkaline. In the TUA3 cell line, the alkalinisation was less pronounced and developed more slowly, reaching 0.4 pH units after 60 min. It then returned more swiftly to the initial value than for the non-transformed WT. Overexpression of OsTTLL12 resulted in a more pronounced alkalinisation of around 0.8 units and a higher residual level after rewarming. Again, the presence of the TUA3 marker slowed the increase in pH and supported its recovery during re-warming. Thus, the overexpression of OsTTLL12 resulted in more pronounced calcium influx under cold stress.

Taken together, overexpression of OsTTLL12 enhanced cold-induced elimination of cortical microtubules, accompanied by a more pronounced calcium influx under cold stress. These differences in early signalling correlated with a reduced cold tolerance, as manifest from a higher mortality under cold stress.

3.3. Overexpression of OsTTLL12 increases stability of cortical microtubules to 1% n-butanol treatment

Phospholipase D (PLD), a 90-kD protein isolated from tobacco membranes has been isolated as linker between plasma membrane and microtubules [7,28] and disruption of PLD signalling by *n*-butanol can mimick the elimination of microtubules in a manner similar to cold stress [8]. Therefore, we wondered whether the effect of *n*-butanol would differ depending on overexpression of OsTTLL12. This was observed, indeed. Compared to the TUA3 marker line, where microtubules were strongly affected, overexpression of OsTTLL12 preserved microtubules under these conditions (Fig. 3c), such that they resembled the situation seen in untreated cells at room temperature (Fig. 3a). Thus, the pattern seen for *n*-butanol was just inversed to that seen for cold stress (Fig. 3b, see also Fig. 2b). If *n*-butanol pre-treatment was combined with cold stress, microtubules were eliminated in both cell lines, whereby in the OsTTLL12 overexpressor some remnants of microtubules could be observed, while in the TUA3 marker line, the GFP signal was diffusely distributed over the entire cytoplasm indicative of a high pool of tubulin heterodimers that were not assembling into microtubules (Fig. 3d). To test, whether the effect of *n*-butanol was due to the dissipation of phosphatidic acid, we also tested *sec*-butanol, which can stimulate PLD activity, but cannot consume the resulting phosphatidic acid [23]. While *sec*-butanol alone did not modulate microtubules in neither cell line (Fig. 3e), it was able to suppress cold induced elimination (Fig. 3f). As a further control, we tested *tert*-butanol, which can neither activate PLD, nor act as acceptor for phosphatidic acid. As expected, this treatment did not exert any effect, neither under room temperature (Fig. 3g), nor under cold stress (Fig. 3h). The microtubules behaved exactly as for the condition without any pre-treatment (room temperature: compare Fig. 3g to Fig. 3a; cold stress: compare Fig. 3h to Fig. 3b). In summary, stimulation of PLD allowing phosphatidic acid to accumulate (*sec*-butanol pre-treatment) stabilised microtubules. Stimulation of PLD, eliminating phosphatidic acid (*n*-butanol pre-treatment), de-stabilised microtubules. While both cell lines behaved in a similar way, if pre-treated by *sec*-butanol, they differed under cold stress and under *n*-butanol treatment. Expression of OsTTLL12 rendered microtubules more susceptible to cold, but more resistant to *n*-butanol. Given the fact that *n*-butanol mimicked the effect of cold upon microtubules, there seems to be a sign reversal with respect to the effect of OsTTLL12 overexpression.

3.4. Rice PLDα1 decorates cortical and mitotic microtubule arrays

In the previous experiment, we had observed that overexpression of OsTTLL12 rendered cortical microtubule more stable against *n*-butanol treatment, indicating a role of a member of the PLD family. Moreover, in a previous work [29], we had co-purified rice PLDα1 together with detyrosinated α-tubulin during EPC affinity chromatography. We

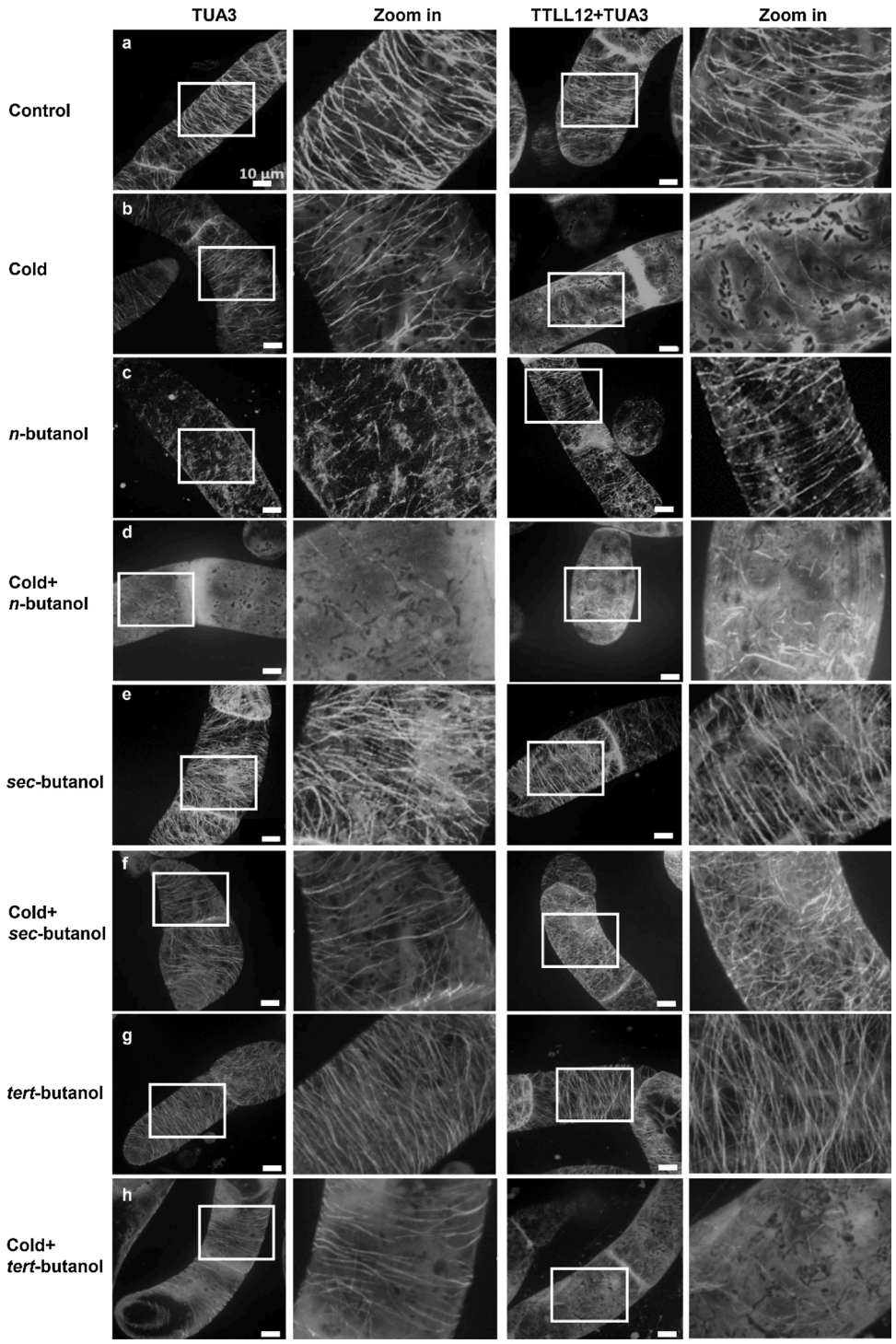

Fig. 3. Microtubular responses in BY-2 cell expressing NtTUA3-GFP (TUA3) and over-expression of OsTTLL12-RFP in NtTUA3-GFP BY-2 cell line (TTLL12 + TUA3) to 1% *n*-butanol, 1% *sec*-butanol or 1% *tert*-butanol treatment either at room temperature or under cold stress (0 °C). a and **b**, microtubular responses under room temperature and cold stress (0 °C) for 15 min, respectively; **c**, **e** and **g**, microtubular responses to 1% *n*-butanol, 1% *sec*-butanol and 1% *tert*-butanol treatment for 60 min under room temperature, respectively; **d**, **f** and **h**, microtubular responses to cold stress (0 °C) in 15 min after pretreatment with 1% *n*-butanol, 1% *sec*-butanol and 1% *tert*-butanol for 30 min, respectively. Zoom in represents the enlargement of rectangle part in the right lane, respectively.

wondered whether PLDα1 interacts with detyrosinated α-tubulin. For this purpose, we cloned rice PLDα1, generated a GFP fusion of it and overexpressed this fusion in BY-2 cells and also used a rice line over-expressing OsPLDα1 fused with GFP to test, whether OsPLDα1 decorates microtubules upon immunofluorescence staining with a monoclonal α-tubulin antibody (Fig. 4). Using tobacco BY-2 cells as model for cycling cells, we could see OsPLDα1 bound to spindle microtubules during metaphase, and phragmoplast microtubules during telophase (Fig. 4A). The GFP signal reporting OsPLDα1 decorated microtubules like beads on a string. The spacing of the signals was very dense, leading to an almost continuous coverage. We further investigated the situation for cortical microtubules in the homologous system (rice) using epidermal cells of the seminal root as model (Fig. 4B). Here, we observed a very close co-localisation as well, albeit the punctate nature of the GFP signal was more evident than for the mitotic microtubule arrays. Overall, OsPLDα1 was tightly matching microtubules both, for cycling and for interphase cells.

3.5. *Overexpression of Rice PLDα1 increases abundance of detyrosinated α-tubulin*

Since OsPLDα1 associated with microtubules and rendered them

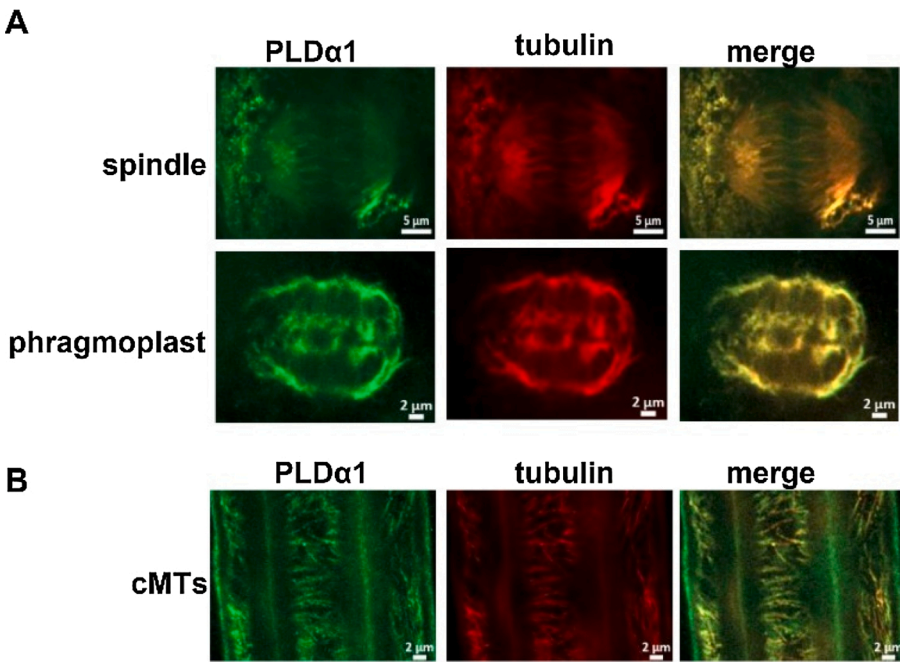

Fig. 4. Subcellular localisation of OsPLDα1 in cycling and non-cycling cells. A, Double-staining of OsPLDα1 in BY-2 cells overexpressing OsPLDα1-GFP in relation to different mitotic microtubule arrays (spindle and phragmoplast). **B**, Double staining of OsPLDα1 in epidermal cells of the rice seminal root in a line overexpressing OsPLDα1-GFP. Microtubules were visualised by immunofluorescence using a monoclonal antibody against detyrosinated α-tubulin (DM1A), and a TRITC-conjugated secondary antibody; OsPLDα1 is reported by the GFP-signal, overlap of both signals in the merged image is indicated by a yellow colour. (For interpretation of the references to colour in this Figure legend, the reader is referred to the web version of this article).

more stable, we wondered, whether overexpression of this protein would modulate the abundance of detyrosinated α-tubulin. In fact, a Western blot analysis probed with monoclonal antibodies against tyrosinated and detyrosinated α-tubulin showed a significant increase in the signal of detyrosinated α-tubulin in BY-2 cells overexpressing OsPLDα1-GFP in comparison with the non-transformed WT (Fig. 5A and B) while the signal of tyrosinated α-tubulin remained unaltered. This was further confirmed by the control of the signals of β-tubulin (Fig. 5C), where overexpressing OsPLDα1-GFP did not affect the abundance of β-tubulin compared with the non-transformed WT either. Thus, OsPLDα1 increased microtubule stability and the abundance of detyrosinated tubulin in the same manner as OsTTLL12 did, leading to the question, whether there is a link between tubulin abundance and microtubule stability.

3.6. Overexpression of OsTTLL12 increases the abundance of NtTUA3-GFP protein

To further test whether overexpression of OsTTLL12 would increase detyrosinated α-tubulin (which might be the cause for the higher stability of microtubules upon *n*-butanol treatment), we conducted a Western blot analysis probing for tyrosinated (Fig. 6B) and detyrosinated (Fig. 6C) α-tubulin by using the monoclonal antibodies ATT and DM1A, respectively [18], and comparing equally loaded total extracts from TUA3 and TTLL12 + TUA3 cells (Fig. 6A). While neither the bands around 50 kDa reporting tyrosinated (Fig. 6B), nor those reporting detyrosinated (Fig. 6C) α-tubulin were showing any significant differences between the two cell lines, both antibodies visualised an additional band at approximately 80 kDa, which was significantly more prounounced in the TTLL12 + TUA3 over the TUA3 cell line (Fig. 6B, C). This was further confirmed by the amount of β-tubulin detected by monoclonal antibody DM1B, where the signal of β-tubulin showed no significant differences between TUA3 and TTLL12 + TUA3 cells (Fig. 6D). Since the apparent molecular weight of GFP is around 28 kDa and tobacco α- tubulin 3 (NtTUA3) is around 55 kDa, it was assumed that this 80 kDa protein band might be the product of transgene NtTUA3-GFP. To verify this, the same lanes were also probed using a monoclonal antibody directed against a C-terminal peptide that is specific for GFP. As expected, this antibody visualised a band at ~30 kDa, well matching with the 28 kDa expected for free GFP (Fig. 6E). The specificity of this antibody was further supported by the fact that it did not pick up the TTLL12-RFP fusion (predicted to be 126 kDa). Similairly to the two α-tubulin antibodies, this anti-GFP antibody detected a band around 80 kDa, which was, again, more pronounced in the TTLL12 + TUA3 double transformed cells and, thus, most likely seems to be the NtTUA3-GFP fusion protein (Fig. 6B). In addition, a band of around 55

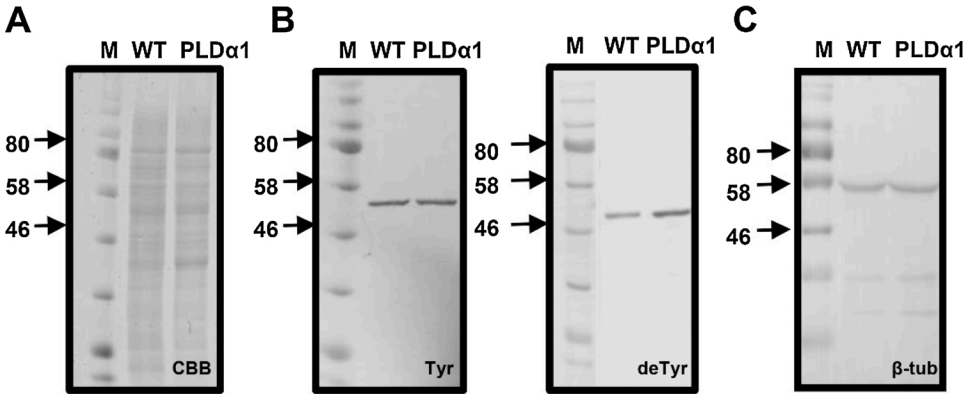

Fig. 5. Abundance of tyrosinated α-tubulin, detyrosinated α-tubulin and β-tubulin in soluble extracts of BY-2 cells overexpressing OsPLDα1-GFP compared to the WT. A, SDS-PAGE gel stained with Coomassie Brilliant Blue (CBB) to show the loading of the lanes. **B** and **C**, detection of tyrosinated (Tyr), detyrosinated α-tubulin (deTyr) and β-tubulin (β-tub) by Western blotting using the monoclonal antibody ATT, DM1A and DM1B, respectively. M, size marker; WT, extracts from non-transformed WT BY-2 cells; PLDα1, extracts from the OsPLDα1-GFP overexpressor line.

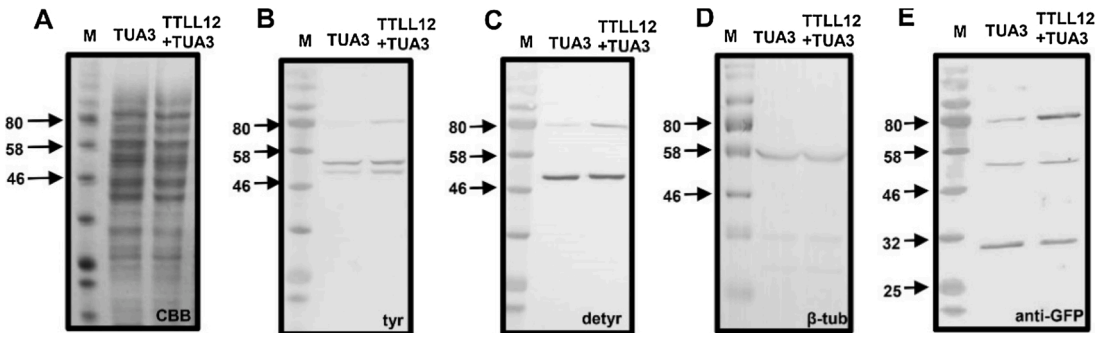

Fig. 6. Abundance of tyrosinated and detyrosinated α-tubulin, β-tubulin as well as of GFP fusions in BY-2 cells expressing NtTUA3-GFP alone (TUA3) or in combination with overexpressed of OsTTLL12-RFP (TTLL12 + TUA3), detected by Western Blot analysis. A, staining with Coomassie Brilliant Blue (CBB) to show equal loading of lanes. Detection of tyrosinated a-tubulin (tyr) with the monoclonal antibody ATT (**B**), detyrosinated a-tubulin (detyr) with the monoclonal antibody DM1A (**C**), β-tubulin (β-tub) with monoclonal antibody DM1B (**D**), and GFP with monoclonal antibody GSN149, against a C-terminal peptide specific for GFP (**E**).

kDa appeared in both samples at similar abundance. Whether this fragment represents a breakdown product of the fusion, where the highly ordered domains (β-sheet cage and chromophore) have been cleaved off, while the flexible and unstructured C-terminal lid [30] harbouring the epitope for the anti-GFP antibody has been retained along with the subsequent tubulin, is not known. Irrespective of the identity of this band, the data suggest that overexpression of OsTTLL12 causes elevated levels of the NtTUA3-GFP fusion, both in tyrosinated and in detyrosinated form.

3.7. *Transcripts for OsTTLL12 and NtTUA3-GFP are mutually stimulated*

To understand, why the NtTUA3-GFP fusion protein becomes more abundant after overexpression of OsTTLL12-RFP, we measured steady-state transcript levels of NtTUA3-GFP in both, the TUA3 and the TTLL12 + TUA3 BY-2 cell line. We found that NtTUA3-GFP transcripts were three times more abundant in the double transformant as compared to the single TUA3 cell line (Fig. 7A). Surprisingly, when we also scored the steady-state levels of the OsTTLL12-RFP transcript, we found it around 20 times higher than that in BY-2 cells overexpressing OsTTLL12-RFP alone (Fig. 7B). It should be noted, however, that the transcript levels of OsTTLL12-RFP were more than an order of magnitude lower than those seen for NtTUA3-GFP. Given the fact that both transgenes were under control of the constitutive CaMV 35S promoter, rather than the endogenous promotor, the expression of the transgene would not be expected to be altered by the presence of a second gene. However, we observed that there is a marked difference in transcript levels depending on the presence or absence of the other transgene, indicative of pronounced post-transcriptional regulation.

3.8. *Oryzalin increases, whereas taxol decreases NtTUA3-GFP transcripts*

To find out whether the elevated transcript levels for NtTUA3 in presence of OsTTLL12-RFP might be caused by a feedback of tubulin heterodimers upon transcript stability, we applied oryzalin to artificially increase the level of non-polymerised tubulin [31]. In fact, oryzalin treatment increase the steady-state level of NtTUA3-GFP in both cell lines (TUA3 and TTLL12 + TUA3). The surplus was around 40 % of the respective value seen without oryzalin, and, thus, more pronounced in the TTLL12 + TUA3 line (Fig. 7C). This result is consistent with a scenario, where the pool of non-assembled tubulin dimers exerts a positive feed-back upon the steady-state transcripts of NtTUA3-GFP. To test this assumption further, we applied taxol as a compound that stabilises microtubules and, thus, decreases the pool of non-assembled tubulin. In fact, treatment with 5 μM taxol decreased the transcripts for NtTUA3-GFP (Fig. 7C). The decrease was around 40 % of the respective value seen without taxol, and, thus, more pronounced in the TTLL12 + TUA3 line. Thus, we see a multiplicative interaction between the effect of the microtubule drugs and the effect of the OsTTLL12-RFP transcript.

3.9. *Cycloheximide increases the steady-state transcripts of NtTUA3-GFP*

The higher transcript levels for NtTUA3-GFP in presence of OsTTLL12-GFP despite the use of the constitutive 35S promoter raised the question, whether this induction requires protein expression. To address this, we used the cycloheximide (CHX), as inhibitor of *de-novo* protein synthesis. We observed that 100 μg/mL CHX (given over 2 h) induced the transcripts of NtTUA3-GFP in both, the TUA3 and the TTLL12 + TUA3 cell lines around two-fold (Fig. 8B). However, the

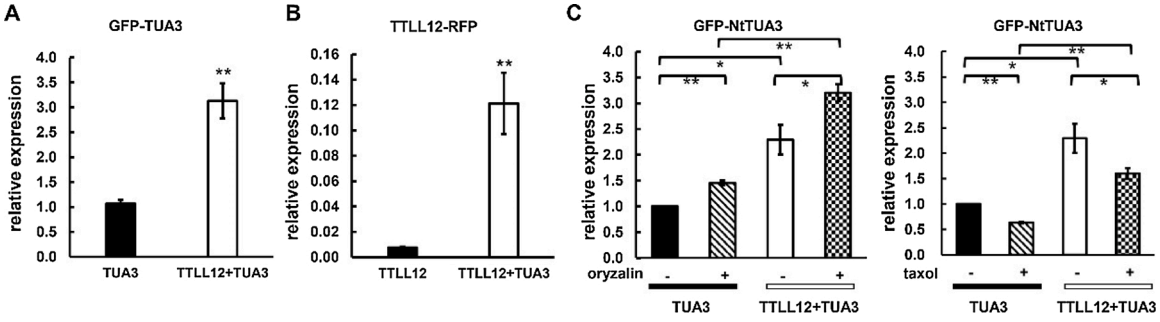

Fig. 7. Steady-state transcript levels of the two transgenes in the NtTUA3-GFP, the OsTTL12-RFP, and the OsTTL12-RFP + NtTUA3-GFP double cell lines. Steady-state transcript levels for GFP-NtTUA3 (**A, C**) and OsTTLL12-RFP (**B**) based on the ΔCt levels in the NtTUA3-GFP line (TUA3), the OsTTLL12-RFP line (TTLL12), and the OsTTLL12-RFP + NtTUA3-GFP double transformant (TTLL12 + TUA3). Note that the scale in **B** is much smaller than in **A**. **C** same condition as in **A**, but after treatment with 5 μM oryzalin (left), or 5 μM taxol (right) for 2 h. Transcripts were measured by real-time qPCR from four biological replicates, each in technical triplicates. Asterisks (*) and (**) indicate significant differences ($P < 0.05$) and ($P < 0.01$) using a Student *t*-test for paired data.

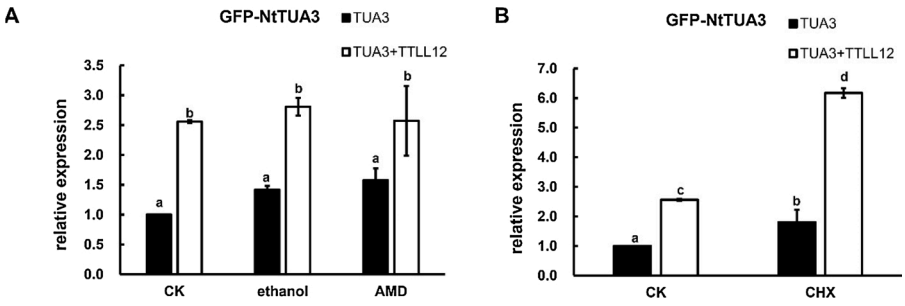

Fig. 8. Dependence of NtTUA3-GFP expression on transcription and translation. Steady-state transcript levels for GFP-NtTUA3 in the GFP-NtTUA3 and the OsTTLL12-RFP + NtTUA3-GFP double transformant (TTLL12 + TUA3) either in untreated cells (control), or after 2 h treatment with 50 μg/mL actinomycin D **(A)**, or 100 μg/mL cycloheximide **(B)**, respectively. CK: control, ethanol: solvent control for the AMD treatment, AMD: actinomycin, CHX: cycloheximide. Transcripts were measured by real-time qPCR from three biological replicates, each in technical triplicates. Different letters (a, b, c and d) indicate significant differences ($P < 0.05$) from LSD test. Transcript levels are given relative to the control value for the GFP-NtTUA3 line.

induction was more substantial in TTLL12 + TUA3 cells, where the resting level was higher as well compared to that in TUA3 cells. In contrast, inhibition of transcription with Actinomycin (Fig. 8A) did not cause significant changes of transcript levels. These results indicated that the steady-state transcript levels of NtTUA3-GFP are negatively regulated by a protein that is relatively short-lived, since blocking protein synthesis over two hours already causes substantial differences.

4. Discussion

In our previous work, we had identified a rice tubulin tyrosine ligase-like 12 (OsTTLL12) protein as the most likely plant homologue for a TTL function, and by overexpression of this OsTTLL12, we could demonstrated that the partitioning between detyrosinated and tyrosinated tubulin was modulated, accompanied by changes in stability and organisation of microtubules [18]. To get more insight into a potential role for tubulin modification for stability-dependent functions of microtubules, we analysed cold sensing which depends on a dynamic sub-population of microtubules [2] and, thus, might serve as sensitive readout. For this purpose, we overexpressed in the current work OsTTLL12-RFP in the background of a microtubule marker line expressing NtTUA3-GFP in tobacco BY-2 cells. We found that OsTTLL12-RFP was present in two pools – one pool was linked with microtubules (all known arrays of plant microtubules were decorated), the other was present as diffuse signal in the cytoplasm (Fig. 1). This second pool could be enhanced by taxol treatment (Supplemental Fig. 1). Since taxol depletes free tubulin dimers, the observed diffuse signals of OsTTLL12-RFP indicated a pool of OsTTLL12-RFP that is not associated with tubulin dimers. Thus, the integration of OsTTLL12 into microtubules does not occur directly, but requires preceding association with tubulin dimers [14]. Furthermore, overexpression of OsTTLL12-RFP amplified cold responses including the rapid alkalinisation of the medium (reporting proton-calcium import), the cold-induced elimination of microtubules, and cold-induced mortality. When we addressed the role of phospholipase D (PLD), as early step of cold signalling, we found significant differences in the responses to different butanols, compounds that can specifically interfere with activation and signal transmission of PLD. Moreover, OsPLDα1, previously identified as protein binding to detyrosinated α-tubulin [29], was found to decorate all microtubule arrays, and the pool of detyrosinated tubulin was increased. Unexpectedly, the overexpression of the two proteins (OsTTLL12-RFP, NtTUA3-GFP) mutually stimulated the accumulation of their transcripts. This prompted us to probe for a potential feedback of the free pool of tubulin heterodimers upon tubulin transcripts, which was confirmed. This feedback was then shown to be amplified by cycloheximide, but also by OsTTLL12-RFP.

These findings stimulate the following questions: 1. What is the role of microtubule-detyrosination for PLD-dependent cold signalling? 2. What can we learn on the feedback of microtubule integrity upon tubulin expression?

4.1. Tubulin tyrosination delineates formative and sensory microtubules

Microtubules have long been known as sensitive target for cold stress mediating the inhibition of cell elongation by cold stress [32]. More recently, they have emerged as a potential regulator for cold tolerance [2,10]. In recent years, an increasing number of studies have shown that the response of microtubules is biphasic. A transient and rapid disassembly of microtubules is thought to be required for activation of signalling. For instance, the ability for cold acclimation in winter wheat correlates with the swift elimination of microtubules during the onset of cold stress, and it is even possible to activate cold acclimation in the absence of cold by a transient elimination of microtubules using propyzamide [3]. As result of successful adaptation, microtubules reassemble and now are endowed with a higher cold stability. Also in the initial sensory phase itself, microtubules differing in their dynamics convey different functions [4]. Stable microtubules help to transfer the force from cold-induced membrane rigidification, whereas dynamic microtubules control the sensitivity of signal perception by restraining the integration of vesicles to plasma membrane. This leads to the question how different degrees of turnover are conferred to different pools of microtubules and raises the importance of stability of microtubules in cold stress signalling. The detyrosination and re-tyrosination of α-tubulin is considered as central factor for (or as central readout of) differential microtubule stability [33]. Our results lend some support to the notion that post-translational modification of tubulin helps to recruit microtubules to different functions:

Firstly, we observed that overexpression of OsTTLL12-RFP rendered microtubules more sensitive to cold stress correlated with rapid depolymerisation (Fig. 2B). This was rescued by $GdCl_3$, the blocker of calcium influx, suggesting that the rapid depolymerisation of microtubules due to overexpression of OsTTLL12-RFP was correlated with calcium influx (Fig. 2D). This result was expected due to the co-transport of protons with calcium, which is the base of the widely used strategy to use extracellular alkalinisation as proxy for calcium influx in response to elicitors, salt and cold stress [8,27,34]. Using the same argument, we conclude from the increase in extracellular alkalinisation that overexpression of OsTTLL12-RFP amplifies cold-induced calcium influx (Fig. 2C). Secondly, we observed a possible functional interaction of tubulin detyrosination with phospholipase D (PLD). The response of microtubules to *n*-butanol, a specific inhibitor of PLD signalling, is altered depending on overexpression of OsTTLL12 (Fig. 3). The specific subtype PLDα1 had been recovered from EPC affinity chromatography by co-elution with detyrosinated α-tubulin in presence of high ionic stringency [29] indicative of specific binding to this modified form of tubulin (while not binding to tyrosinated tubulin, despite the fact that this form was eluted at much lower ionic stringency). We were then able to show that a GFP fusion of OsPLDα1 was decorating microtubules, both in cycling tobacco BY-2 cells as heterologous system and in non-cycling rhizoderm cells of rice itself (Fig. 4). Eventually, we observed that tobacco cells overexpressing OsPLDα1 showed an increase of de-tyrosinated α-tubulin (Fig. 5).

The functional and physical link between PLD and microtubules corrobated by these findings is consistent with the literature record. Plant PLD had been originally identified from tobacco membranes as a linker between plasma membrane and microtubules [7], and has emerged as a signalling hub for stress and phytohormonal signalling, but also for membrane metabolism [2,35]. By cleaving phospholipids to phosphatidic acid (PA), the *Arabidopsis* homologue AtPLDα1 was shown to stabilise microtubules against salt stress by activating the microtubule associated protein MAP65−1 [36]. When PA is consumed by transfer to *n*-butanol as acceptor, microtubules were reported to detach from the plasma membrane [28]. This finding was later questioned by experiments with membrane ghosts, where microtubules remained attached to the membrane [37]. However, the depolymerisation of microtubules by *n*-butanol was confirmed in that study as well, even using *in-vitro*. While these authors had claimed that this indicates a direct disruptive effect of *n*-butanol, this conclusion seems not justified in our opinion, since they used a purification protocol that did not include any separation of MAPs from microtubules, such that their *in-vitro* microtubules would still be decorated with MAPs such PLD. The fact that their disruption *in-vitro* was not seen with *tert*-butanol, a chemically close analogue of *n*-butanol, but not able to accept PA, represents a very specific signature for PLD being involved as well. Irrespective of these details, one can state that our observation that OsTTLL12 renders microtubules resilient against *n*-butanol clearly supports a functional interaction between PLD and cortical microtubules.

4.2. *Microtubules interact differentially with PLD depending on detyrosination*

Our pharmacological mapping of this phenomenon by using different butanols allows some insight into the details of signalling (Fig. 3): The effect on microtubule persistence is opposed for *n*-butanol (stabilisation effect of OsTTLL12) and cold (de-stabilising effect of OsTTLL12). If *n*-butanol is administered prior to cold stress, it amplifies microtubules in response to cold in the absence of OsTTLL12, while it clearly mitigates in presence of OsTTLL12. While the closely related *tert*-butanol does not show any effect, *sec*-butanol does, although it should not be able to accept PA. This seemingly enigmatic finding does not stand alone, however, since *sec*-butanol had already found earlier to modulate the cold response of microtubules in cells of grapevine [8]. These observations can be explained on the mode of action for these butanols [23] (Fig. 9, upper circle): primary alcohols, such as *n*-butanol, can activate a G-protein that in turn activates PLD, which then cleaves phospholipids. The resulting phosphatidic acid (PA) would normally convey the signal generated from the G-protein activation. However, the alcohol that had stimulated the G-protein, also serves as acceptor for PA and, thus, dissipates the signal. Secondary alcohols, such as *sec*-butanol can activate the G-protein as well, but are not able to consume PA, such that they are not expected to disrupt signalling. Tertiary alcohols can neither activate the G-protein, nor accept PA, so they are completely inactive analogues. While we can confirm that *tert*-butanol is completely inactive (Fig. 3g, h), we see a clear activity on the microtubular cold response by

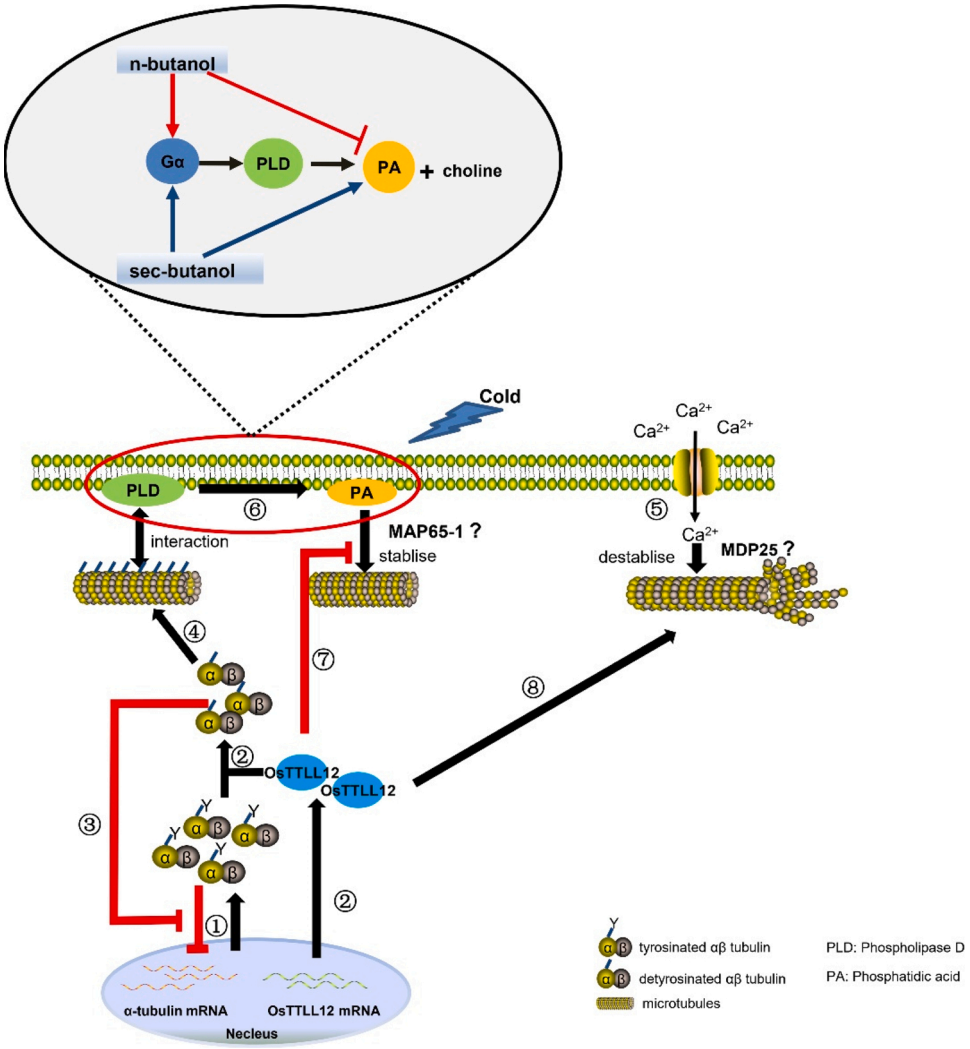

Fig. 9. Proposed Model of tubulin detyrosination in cold signalling and regulation of tubulin synthesis. Amost all plant α-tubulins can be genetically translated with a C-terminal tyrosine and after translation, these tyrosinated αβ tubulin dimers may act as inhibitor to block the translation of α-tubulin mRNA to protein (①), in order to calibrate tubulin accumulations in cytoplasm. When overexpressed OsTTLL12, it firstly accumulates pool of OsTTLL12 and accelerates the process of posttranslational modification, resulting more detyrosinated α-tubulin dimers (②) that in turn diminish the inhibitory of tyrosinated αβ tubulin dimers on the translation of α-tubulin (③) and in other hand interact with phospholipase D (④). Upon cold stress, cold activates Ca^{2+} influx, inducing faster depolymerisation of microtubules (⑤). In parallel, phospholipase D (PLD) can be activated by Gα protein and hydrolyses structural phospholipids to produce phosphatidic acid (PA) and free choline (⑥). Among this process, *n*-butanol and *sec*-butanol both can activate Gα protein and stimulates PLD, while *n*-butanol has an inhibitory effect on the forming of PA and *sec*-butanol promotes PA forming. Overexpression of OsTTLL12 has an inhibitory effect on the PA-dependent microtubule stabilising, probably by preventing the couples of microtubules and MAP65-1, since OsTTLL12 might compete the binding sites of MAP65-1 on microtubules (⑦). In parallel, overexpression of OsTTLL12 promotes the Ca^{2+} induced microtubule destabilising, possibly through the activation of MDP25 that destabilises microtubules (⑧).

sec-butanol. We think that it is not possible to resolve the conundrum on the base of a simplistic model, where PA is the only signal conveying cold stress, but that additional signals need to be considered. We propose a model (Fig. 9), where microtubules might be antagonistically regulated by PA-dependent activation of a stabilising MAP (a good candidate would be MAP65−1, which is activated by PA [36]), and the calcium-dependent activity of a destabilising MAP (a good candidate would be MDP25 [38], which has been shown to overrun the stabilising effect of MAP65−1 *in vitro* [39]). These interactions might be modulated by OsTTLL12. In our previous study, we showed that overexpression of OsTTLL12 increases the abundance of detyrosinated tubulin [18], which will increase the interaction with PLD [29] (Fig. 5). At the same time PLD will promote the activity of OsTTLL12 leading to higher levels of detyrosinated tubulin (Fig. 5). One reason why we consider MAP65−1 as possible candidate is the fact that MAP65−1 binds to the C-terminus of α-tubulin [40], *i.e.* the site where OsTTLL12 might act and, therefore, bind, such that both proteins might also compete for the binding site of C-terminus of α-tubulin [18]. As a result, OsTTLL12 might uncouple microtubules from MAP65−1.

If our hypothesis holds true, using this model, it is possible to spell out our complex patterns: Since *n*-butanol consumes PA, it is expected to lower the activity of MAP65−1, leading to microtubule elimination. Our model predicts that the presence of OsTTLL12 is expected to partially uncouple microtubules from the activities of MAP65−1, such that they are now more persistent as compared to the situation, where OsTTLL12 is missing (Fig. 3c). Similarly to *n*-butanol, cold activates PLD within minutes [41], which should increase the steady-state level of PA and increase the stabilising activity of MAP65−1 leading to stable microtubules. However, our observations contradict this implication, because we see that microtubules are eliminated. We have shown earlier that cold-induced elimination of microtubules requires calcium influx [8], and we see now that a block of calcium influx by $GdCl_3$ can suppress cold-induced microtubules (Fig. 2D). We propose therefore that microtubule-destabilising MAPs that are activated by calcium are relevant here. The primary candidate would be MDP25 [38]. This protein is linked to the membrane through N-terminal myristoylation [42], and might, therefore, interfere with other membrane-microtubule interactions, such as those between PLD and detyrosinated microtubules, which would explain, why the cold-dependent elimination is more prominent in presence of OsTTLL12 (Fig. 3b, and Fig. 3h). When *n*-butanol is administered prior to cold stress, the steady-state level of PA is not only strongly reduced, but also has no way to increase in response to cold, because any PA generated in response to the cold activation of the G-protein, would be immediately consumed. This should basically eliminate the activity of MAP65−1, rendering microtubules more susceptible to the cold-induced effect of MDP25, which is consistent with our observation (Fig. 3d). Again, OsTTLL12 should theoretically mitigate this, because it might uncouple microtubules from MAP65−1, which is also consistent with our observation (Fig. 3f). Pre-incubation with *sec*-butanol is supposed to activate the G-protein leading to a higher steady-state level of PA (which is not consumed now, because *sec*-butanol cannot accept it). This should activate MAP65−1 beyond the usual level and cause microtubule bundling. This is a non-intuitive implication of our model and matches exactly our observation (compare Fig. 3g to Fig. 3a). However, a subsequent cold stress should counteract this through the calcium-dependent activation of MDP25. This implication as well is congruent with our observations (Fig. 3h). In the presence of OsTTLL12, both, the microtubule bundling (in response to *sec*-butanol alone), as well as the microtubule elimination (in response to *sec*-butanol followed by cold) should be less pronounced, due to the possible uncoupling from MAP65. This is again, consistent with our observations (Fig. 3e, f).

In summary, we propose that post-translational modification of α-tubulin delineates two pools of microtubules that probably interact differentially with signalling (PLD, PA), and with microtubule-associated proteins that, depending on signalling, eliminate or stabilise microtubules, respectively. By spelling out the implications of this model, we can explain even non-intuitive results from our pharmacological interference.

4.3. Tubulin detyrosination – a determinant of tubulin synthesis?

Modulations of microtubule turnover have a direct impact on the steady-state level of soluble tubulin heterodimers. The pool of non-polymerised tubulin must be tightly regulated – if it is too low, this would impair the ability of the cytoskeleton for remodelling, if it is too high, it would impair viability, because the self-organisation of microtubules requires competition of different nucleation sites for a limited pool of heterodimers [43]. In fact, attempts to overexpress tubulin in different organisms were in most cases to no avail, because the surplus of the exogenous tubulin was compensated by a corresponding suppression of endogenous tubulin. A very impressive example has been the attempt to overexpress a mutated tubulin with an altered binding site for dinitroanilines, which was attempted in maize [44]. Not a single transformant was recovered, where the abundance of α-tubulins dominated over that of β-tubulin, which means that there must be a feedback from the pool of dimers upon the expression of tubulin genes. This feedback seems to act on the level of posttranscriptional regulation [45,46].

It seems that the overexpression of OsTTLL12 interferes with this feedback (Fig. 9), and in the following we try to use this phenomenon to infer several features on this feedback.

Since overexpression of OsTTLL12 in tobacco BY-2 cells increases the abundance of the co-expressed GFP-NtTUA3, both, at the protein level and the transcript level (Figs. 6 and 7A), although both transgenes are driven by the constitutive CaMV 35S promoter, there must be post-transcriptional regulation. In fact, the amplification of the tubulin-GFP fusion transcripts was not modulated by the transcription blocker actinomycin, while the translation blocker cycloheximide even amplified the steady-state transcript levels for GFP-NtTUA3 in the double overexpressor line (Fig. 8). Thus, the observed modulation of transcript levels depends on a factor that requires translation and might be linked with the pool of non-assembled tubulin heterodimers.

Indeed, the feedback from the non-assembled pool of tubulin dimers upon tubulin transcripts is well known from mammalian cells. If this pool is increased by colchicine or by microinjection of tubulin, the excess dimers bind to the *statu nascendi* β-tubulin protein by virtue of a MREI motif conserved in the N-terminus of β-tubulin resulting in arrested translation and degradation of tubulin mRNA [47,48]. A second feedback mechanism involves the binding of α-tubulin to α-tubulin mRNA through a secondary structure in the 5′ untranslated region (UTR), again leading to inhibition of tubulin translation and subsequent degradation of tubulin transcripts [49]. Whether these mechanisms exist in plants, is not known, but the MREI motif is also found in β-tubulins from plants and differential degradation of specific β-tubulin transcripts has been demonstrated in a defence context for suspension cells of soybean [50].

However, our results are not explained by such a negative feedback of the non-assembled tubulin pool upon the steady-state level of tubulin transcripts. When we increase the soluble tubulin pool by pre-treatment with oryzalin (Fig. 7C), we see *more*, and not *less* transcripts of GFP-tubulin fusion. Conversely, when we reduce the pool of soluble tubulin by taxol, we see *less*, and not *more* transcripts of GFP-tubulin fusion (Fig. 7D). Also, the fact that overexpression of OsTTLL12 can increase the abundance of the GFP-tubulin fusion, both on the protein (Fig. 6) and on the transcript level (Fig. 7) is not compatible with a scenario in which non-assembled tubulin blocks transcripts. In our previous work [18], we observed that overexpression of OsTTLL12 shifts tubulin into the detyrosinated state linked with a higher resistance to oryzalin, indicative for higher stability of microtubules, *i.e.*, with a lower level of non-assembled tubulin. Again, we do not see the reduction of tubulin transcripts and fusion protein inferred from a negative feedback of dimers on transcript levels. Instead, we see a clear induction. It should

be noted that overexpression of OsTTLL12 increased the level of GFP-NtTUA3, without affecting the endogenous tubulins level (Fig. 6). The GFP fusion is located at the N-terminal of NtTUA3, and the N-terminal fusion of GFP has been reported to interfere with the GTPase function that inhibits GTP hydrolysis, thus leading to polymerisation-prone microtubules with a longer lifetime [51]. Therefore, the OsTTLL12 is expected to act on the GFP-fused tubulin more efficiently as compared to the endogenous tubulins.

It is possible, though, to reconcile our data with the negative feedback model by introducing a small, but decisive addition. If it were not just *any* tubulin heterodimer that can block translation, but just a heterodimer containing tyrosinated α-tubulin that can act as inhibitor, it is possible to reach congruence between model and data (Fig. 9). The increase of tubulin dimers in response to oryzalin is coming from microtubule treadmilling, *i.e.*, those dimers had a "history" of being incorporated in microtubules, which means that they are preferentially detyrosinated, because TTC acts post assembly [15]. These dimers originate, therefore, mainly from the proximal part of microtubules, which are preferentially detyrosinated [52]. The same holds true when we block translation by cycloheximide, which will reduce the pool of nascent (tyrosinated) tubulin. Similarly, since overexpress OsTTLL12 mainly shifts tubulins into the detyrosinated form [18] (as also observed in Fig. 6C with an increase in detyrosinated GFP-fused tubulin due to overexpression of OsTTLL12), we should expect an increase of transcript levels as well, which is, what we observe (Fig. 7B). Instead, treatment with taxol will suppress treadmilling and, thus, reduce the pool of detyrosinated tubulin dimers, which makes it more likely that the tubulin dimer hitting a ribosome harbours tyrosinated α-tubulin, such that transcript levels should drop, which is, what we observe. Since in mammalian cells, the fraction of detyrosinated tubulin is very small, less than 2% [15], the difference between the tubulin forms with respect to this feedback will be hardly detectable. However, in plant cells, where the fraction of detyrosinated tubulin is far more relevant, this difference will become manifest, which is exactly, what we observe.

5. Conclusions and outlook

While the strict conservation of the C-terminal tyrosine is valid for plants as well, the functional relevance of this phenomenon has remained elusive in plants. Extending our previous functional analysis of the only *bona-fide* candidate in rice for tubulin modification, OsTTLL12, we show in the current work that this protein is linked with a functional differentiation of microtubules. We show that detyrosinated microtubules interact with phospholipase D (PLD), which is modulating cold sensing. In addition, we discovered a feedback of detyrosination on tubulin transcripts, arriving at a model where a subset of soluble heterodimers (those harbouring tyrosinated α-tubulin) is reducing the steady-state levels of tubulin transcripts. Thus, post-translational modification partitions two functionally different pools of α-tubulin: naïve tubulin (which is tyrosinated) *versus* tubulin with a history of having passed through a microtubule (which is detyrosinated). However, these results also open many questions: While OsTTLL12 rather promotes detyrosinated tubulin, there is no other evident candidate that might act as tyrosine ligase. Is it conceivable that this protein exerts different functions dependent on complexation with different accessory proteins? What is the structural base for the differential interaction of different α-tubulin pools with tubulin transcripts? Why are the transcript levels of OsTTLL12 increased in the background of the GFP-tubulin marker line? To address these questions will require recombinant expression of OsTTLL12 in a soluble form, which is the topic of ongoing work. Furthermore, what is the structural base of the interaction between PLD and de-tyrosinated α-tubulin? Does this interaction depend on additional modifiers? Pull-downs (*in vitro*) or Bimodal fluorescence complementation or FRET assays (*in vivo*) would allow to test the physical interaction between PLD and detyrosinated α-tubulin. To follow the interaction of PLD and OsTTLL12-RFP in relation to microtubules in response to cold stress, a triple line expressing fluorescently tagged PLD in the background of the OsTTLL12-RFP and TUA3-GFP double expressor, would be an interesting tool. To generate such a tool represents a certain challenge though. Last, but not least, future study should establish a way to quantify the composition of free tubulin dimers and tubulins on microtubules, which will provide a way to study how tubulin expression is tightly controlled by microtubule dynamics in responses to cold stress.

Author contributions statement

KZ, WS, XZ, XL and DH performed the primary experimental work. KZ and WS generated the overexpression of OsTTLL12-RFP in NtTUA3-GFP BY-2 cell line. KZ, LW, MR and PN evaluated experimental design and performed data interpretation. KZ drafted the manuscript and PN edited the manuscript and developed the conceptual framework. All authors read and approved of the content.

Declaration of Competing Interest

The authors declare no conflict of interest.

Acknowledgements

We thank Sabine Purper (Molecular Cell Biology, Botanical Institute, KIT) for technical assistance in BY-2 cell culture. Thanks for Prof. Wenhua Zhang and Prof. Wenqiang Tang kindly providing the seeds of overexpression of OsPLDα1-GFP rice line. This work was supported by a fellowship from the Chinese Scholarship Council to Kunxi Zhang.

Appendix A. Supplementary data

Supplementary material related to this article can be found, in the online version, at doi:https://doi.org/10.1016/j.plantsci.2021.111155.

References

[1] T. Hashimoto, Microtubules in plants, Arab. Book/Am. Soc. Plant Biol. 13 (2015).
[2] L. Wang, E. Sadeghnezhad, P. Nick, Upstream of gene expression: what is the role of microtubules in cold signalling? J. Exp. Bot. 71 (2020) 36–48.
[3] A. Abdrakhamanova, Q.Y. Wang, L. Khokhlova, P. Nick, Is microtubule disassembly a trigger for cold acclimation? Plant Cell Physiol. 44 (2003) 676–686.
[4] L. Wang, E. Sadeghnezhad, M. Riemann, P. Nick, Microtubule dynamics modulate sensing during cold acclimation in grapevine suspension cells, Plant Sci. 280 (2019) 18–30.
[5] T. Hamada, Microtubule-associated proteins in higher plants, J. Plant Res. 120 (2007) 79–98.
[6] J. Marc, D.E. Sharkey, N.A. Durso, M. Zhang, R.J. Cyr, Isolation of a 90-kD microtubule-associated protein from tobacco membranes, Plant Cell 8 (1996) 2127–2138.
[7] J.C. Gardiner, J.D. Harper, N.D. Weerakoon, D.A. Collings, S. Ritchie, S. Gilroy, R. J. Cyr, J. Marc, A 90-kD phospholipase D from tobacco binds to microtubules and the plasma membrane, Plant Cell 13 (2001) 2143–2158.
[8] L. Wang, P. Nick, Cold sensing in grapevine—which signals are upstream of the microtubular "thermometer", Plant Cell Environ. 40 (2017) 2844–2857.
[9] Q. Zhang, P. Song, Y. Qu, P. Wang, Q. Jia, L. Guo, C. Zhang, T. Mao, M. Yuan, X. Wang, Phospholipase Dδ negatively regulates plant thermotolerance by destabilizing cortical microtubules in Arabidopsis, Plant, Cell Environ. 40 (2017) 2220–2235.
[10] P. Nick, Microtubules, signalling and abiotic stress, Plant J. 75 (2013) 309–323.
[11] K. Ersfeld, J. Wehland, U. Plessmann, H. Dodemont, V. Gerke, K. Weber, Characterization of the tubulin-tyrosine ligase, J. Cell Biol. 120 (1993) 725–732.
[12] A. Akhmanova, H. Maiato, Closing the tubulin detyrosination cycle, Science 358 (2017) 1381–1382.
[13] J. Nieuwenhuis, A. Adamopoulos, O.B. Bleijerveld, A. Mazouzi, E. Stickel, P. Celie, M. Altelaar, P. Knipscheer, A. Perrakis, V.A. Blomen, Vasohibins encode tubulin detyrosinating activity, Science 358 (2017) 1453–1456.
[14] N. Kumar, M. Flavin, Preferential action of a brain detyrosinolating carboxypeptidase on polymerized tubulin, J. Biol. Chem. 256 (1981) 7678–7686.
[15] G.G. Gundersen, S. Khawaja, J.C. Bulinski, Postpolymerization detyrosination of alpha-tubulin: a mechanism for subcellular differentiation of microtubules, J. Cell Biol. 105 (1987) 251–264.
[16] B. Wiesler, Q.Y. Wang, P. Nick, The stability of cortical microtubules depends on their orientation, Plant J. 32 (2002) 1023–1032.

[17] C. Janke, The tubulin code: molecular components, readout mechanisms, and functions, J. Cell Biol. 206 (2014) 461–472.
[18] K. Zhang, X. Zhu, S. Durst, P. Hohenberger, M.-J. Han, G. An, V.P. Sahi, M. Riemann, P. Nick, A rice tubulin tyrosine ligase-like 12 protein affects the dynamic and orientation of microtubules, J. Integr. Plant Biol. 63 (2021) 848–864.
[19] F. Kumagai, A. Yoneda, T. Tomida, T. Sano, T. Nagata, S. Hasezawa, Fate of nascent microtubules organized at the M/G1 interface, as visualized by synchronized tobacco BY-2 cells stably expressing GFP-tubulin: time-sequence observations of the reorganization of cortical microtubules in living plant cells, Plant Cell Physiol. 42 (2001) 723–732.
[20] C. Huo, B. Zhang, H. Wang, F. Wang, M. Liu, Y. Gao, W. Zhang, Z. Deng, D. Sun, W. Tang, Comparative study of early cold-regulated proteins by two-dimensional difference gel electrophoresis reveals a key role for phospholipase Dα1 in mediating cold acclimation signaling pathway in rice, Mol. Cell Proteomics 15 (2016) 1397–1411.
[21] O. Bensaude, Inhibiting eukaryotic transcription. Which compound to choose? How to evaluate its activity? which compound to choose? how to evaluate its activity? Transcription 2 (2011) 103–108.
[22] F. Waller, M. Furuya, P. Nick, OsARF1, an auxin response factor from rice, is auxin-regulated and classifies as a primary auxin responsive gene, Plant Mol. Biol. 50 (2002) 415–425.
[23] T. Munnik, S.A. Arisz, T. De Vrije, A. Musgrave, G protein activation stimulates phospholipase D signaling in plants, Plant Cell 7 (1995) 2197–2210.
[24] K.J. Livak, T.D. Schmittgen, Analysis of relative gene expression data using real-time quantitative PCR and the $2^{-\Delta\Delta CT}$ method, Methods 25 (2001) 402–408.
[25] G.W. Schmidt, S.K. Delaney, Stable internal reference genes for normalization of real-time RT-PCR in tobacco (Nicotiana tabacum) during development and abiotic stress, Mol. Genet. Genomics 283 (2010) 233–241.
[26] L. Thion, C. Mazars, P. Thuleau, A. Graziana, M. Rossignol, M. Moreau, R. Ranjeva, Activation of plasma membrane voltage-dependent calcium-permeable channels by disruption of microtubules in carrot cells, FEBS Lett. 393 (1996) 13–18.
[27] G. Felix, J.D. Duran, S. Volko, T. Boller, Plants have a sensitive perception system for the most conserved domain of bacterial flagellin, Plant J. 18 (1999) 265–276.
[28] P. Dhonukshe, A.M. Laxalt, J. Goedhart, T.W. Gadella, T. Munnik, Phospholipase D activation correlates with microtubule reorganization in living plant cells, Plant Cell 15 (2003) 2666–2679.
[29] J. Krtková, A. Zimmermann, K. Schwarzerová, P. Nick, Hsp90 binds microtubules and is involved in the reorganization of the microtubular network in angiosperms, J. Plant Physiol. 169 (2012) 1329–1339.
[30] M.W. Lassalle, S. Kondou, Uncovering the role of the flexible C-terminal tail: a model study with Strep-tagged GFP, Biochim. Open. 2 (2016) 1–8.
[31] S. Gianì, X. Qin, F. Faoro, D. Breviario, In rice, oryzalin and abscisic acid differentially affect tubulin mRNA and protein levels, Planta 205 (1998) 334–341.
[32] M. Sakiyama, H. Shibaoka, Effects of abscisic acid on the orientation and cold stability of cortical microtubules in epicotyl cells of the dwarf pea, Protoplasma 157 (1990) 165–171.
[33] L. Parrotta, M. Cresti, G. Cai, Accumulation and post-translational modifications of plant tubulins, Plant Biol. 16 (2014) 521–527.
[34] A. Ismail, M. Seo, Y. Takebayashi, Y. Kamiya, E. Eiche, P. Nick, Salt adaptation requires efficient fine-tuning of jasmonate signalling, Protoplasma 251 (2014) 881–898.
[35] B.O. Bargmann, T. Munnik, The role of phospholipase D in plant stress responses, Curr. Opin. Plant Biol. 9 (2006) 515–522.
[36] Q. Zhang, F. Lin, T. Mao, J. Nie, M. Yan, M. Yuan, W. Zhang, Phosphatidic acid regulates microtubule organization by interacting with MAP65-1 in response to salt stress in Arabidopsis, Plant Cell 24 (2012) 4555–4576.
[37] A. Hirase, T. Hamada, T.J. Itoh, T. Shimmen, S. Sonobe, n-Butanol induces depolymerization of microtubules in vivo and in vitro, Plant Cell Physiol. 47 (2006) 1004–1009.
[38] J. Li, X. Wang, T. Qin, Y. Zhang, X. Liu, J. Sun, Y. Zhou, L. Zhu, Z. Zhang, M. Yuan, MDP25, a novel calcium regulatory protein, mediates hypocotyl cell elongation by destabilizing cortical microtubules in Arabidopsis, Plant Cell 23 (2011) 4411–4427.
[39] T. Qin, J. Li, M. Yuan, T. Mao, Characterization of the role of calcium in regulating the microtubule-destabilizing activity of MDP25, Plant Signal. Behav. 7 (2012) 708–710.
[40] C. Wicker-Planquart, V. Stoppin-Mellet, L. Blanchoin, M. Vantard, Interactions of tobacco microtubule-associated protein MAP65-1b with microtubules, Plant J. 39 (2004) 126–134.
[41] E. Ruelland, C. Cantrel, M. Gawer, J.-C. Kader, A. Zachowski, Activation of phospholipases C and D is an early response to a cold exposure in Arabidopsis suspension cells, Plant Physiol. 130 (2002) 999–1007.
[42] S. Vosolsobě, J. Petrášek, K. Schwarzerová, Evolutionary plasticity of plasma membrane interaction in DREPP family proteins, Biochim. Biophys. Acta Biomembr. 1859 (2017) 686–697.
[43] P. Nick, Mechanics of the cytoskeleton. Mechanical Integration of Plant Cells and Plants, Springer, 2011, pp. 53–90.
[44] R.G. Anthony, P.J. Hussey, Suppression of endogenous α and β tubulin synthesis in transgenic maize calli overexpressing α and β tubulins, Plant J. 16 (1998) 297–304.
[45] D. Breviario, P. Nick, Plant tubulins: a melting pot for basic questions and promising applications, Transgenic Res. 9 (2000) 383–393.
[46] D. Breviario, S. Gianì, L. Morello, Multiple tubulins: evolutionary aspects and biological implications, Plant J. 75 (2013) 202–218.
[47] D.W. Cleveland, Autoregulated instability of tubulin mRNAs: a novel eukaryotic regulatory mechanism, Trends Biochem. Sci. 13 (1988) 339–343.
[48] D.W. Cleveland, M.F. Pittenger, J.R. Feramisco, Elevation of tubulin levels by microinjection suppresses new tubulin synthesis, Nature. 305 (1983) 738–740.
[49] M.L. Gonzalez-Garay, F. Cabral, Alpha-tubulin limits its own synthesis: evidence for a mechanism involving translational repression, J. Cell Biol. 135 (1996) 1525–1534.
[50] C. Ebel, L.G. Gómez, A.-C. Schmit, G. Neuhaus-Url, T. Boller, Differential mRNA degradation of two β-tubulin isoforms correlates with cytosolic Ca^{2+} changes in glucan-elicited soybean cells, Plant Physiol. 126 (2001) 87–96.
[51] T. Abe, T. Hashimoto, Altered microtubule dynamics by expression of modified α-tubulin protein causes right-handed helical growth in transgenic Arabidopsis plants, Plant J. 43 (2005) 191–204.
[52] Y. Song, S.T. Brady, Post-translational modifications of tubulin: pathways to functional diversity of microtubules, Trends Cell Biol. 25 (2015) 125–136.